Examining the Frictional Behavior of Primitive Contact Geometries for use as Robotic Finger Pads

Michael T. Leddy, *Student Member, IEEE* and Aaron M. Dollar, *Senior Member, IEEE*

Abstract— Prosthetic and robotic grippers rely on soft finger pads to better acquire objects of varying size, shape and surface. However, the frictional behavior of soft finger pads of different designs and geometries have yet to be quantitatively compared, in large part due to the difficulty in modeling soft contact mechanics. In this paper, we experimentally examine the frictional behavior of several common primitive contact geometries in terms of their performance under shear loads that would tend to cause the contact to slip and the grasp to potentially fail. Finger pads were fabricated and varied in size and geometry, all normalized to the human finger pad contact area under various contact orientations. The effective static and kinetic coefficients of friction were recorded for each finger pad under a range of common grasping loads. The results show that the variance in contact curvature, contact patch geometry and pressure distribution have influences on key parameters for grasping at low forces. The advantages and disadvantages of these simple geometries are discussed for design of single finger, multi-finger and manipulation-based robotic hands.

I. INTRODUCTION

General-purpose robotic and prosthetic hands and grippers typically utilize a small set of common fingertip designs: hemispherical, flat, or cylindrical [1-3]. These common geometries, the underlying structure generally fabricated from smooth metals or plastic, are often covered with soft rubber-like finger pads to improve the stability of the contact through high friction [4]. However, the performance of these basic fingertip and finger pad geometries have yet to be quantitatively analyzed and compared to one another. In this paper, we experimentally compare the frictional performance of these three basic finger pad geometries as a function of their size, contact geometry and loading conditions.

The effectiveness of soft elastic finger pads in grasping environments is dependent on the object stability maintained while grasping. The local contact geometry and friction coefficient are key aspects to determining the stability of an antipodal precision grasp or multi-contact wrap grasp used commonly in modern robotic hands [4]. To ensure that the grasp of an object remains stable, the hand-object system must remain stable by either satisfying force closure [5] or by sufficiently caging the object within the gripper [6]. Simple point contact coulomb friction models are generally sufficient for determining object stability for contact between a rigid finger and object. However, this is complicated in elastic models where contact is distributed over an area and pressure distributions can be non-uniform. Hertzian contact mechanics initially focused heavily on frictionless relationships,
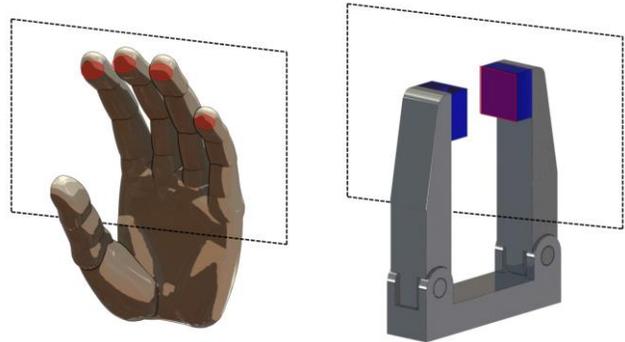
Figure 1. The elastic contact regions of a human hand and a robotic parallel jaw gripper with artificial finger pads on a planar surface.

analyzing the close-form solution of stresses and displacements to linear elasticity equations [7], which alongside experimentation led to several models that can describe frictional properties of soft materials [8]. Although there has been significant progress in the modeling of elastic contact [9-10], the approaches taken are still very much incomplete and require significant computational time for simple structures. Furthermore, the complexities and uncertainty in robotic grasping have proved to be an additional challenge for designing generalizable soft finger pads.

Many experimental approaches have been made to fabricate effective finger pads for robotic hands to overcome the difficulty of modeling soft contacts. Designs are split between complex finger pads that are experimentally optimized for a discrete subset of objects or tasks [11-12], or simple geometric shapes, that provide an intuitive framework for grasping [1-3], planning [13] and learning [14]. These finger pads, primitive or complex, are either iterated through virtual evaluation or experimental evaluation. For virtual evaluation, a set of virtual objects in the form of point clouds or tessellated surfaces are first simulated [15]. These virtual objects are used to plan antipodal grasps for parallel or multi-fingered grasps [13-14] during the finger pad optimization. When creating optimal finger pads given specific gripper kinematics, the goal is to maximize the contact and force between local object geometry and finger pad geometry [6] [16-17]. Similarly, in an experimental setting a finger pad is produced and a sample set of objects are grasped. The effectiveness of the gripper is determined by the amount of objects the gripper can successfully pick and place, nominally using a multi-fingered hand and a robotic arm [17-18]. However, there is limited research evaluating the performance of finger pads alone, the analysis of which is necessary for creating more advanced grippers architectures.

In this paper, we set out to experimentally compare the frictional properties of three common finger pad shape primitives seen in research and commercial hands [1-3]. Due to the variability in gripper kinematics, architecture, and object geometry seen in robotic grasping applications, we use a simplified experimental framework consisting of a single contact loaded vertically on a flat contact surface mounted to a high-resolution force sensor. This contact surface is then displaced laterally, and the normal and tangential force profiles are recorded, from which effective coefficients of static and kinetic friction are calculated. The finger pad sizes are selected such that they produce contact areas matching those of the human index finger at three different orientations. The performance of these grip pads were then compared to each other and the human finger pad to provide insight into developing effective artificial finger pad geometries for robotic grasping applications.

II. METHODS

In this section we will discuss the methods used to both create and evaluate the primitive robotic finger pad geometries. First, a pipeline was developed to accurately measure the contact area of a human participant's index finger in a variety of orientations. Next, robotic finger pads characterized by their largest linear dimension producing a circular, rectangular and square contact area were fabricated that aligned with these contact areas at a given load. Last, an ASTM standard test [18] was used to determine the effective coefficients of friction and holding pressure of the fabricated grip pads over a range of loads common to human and robotic grasping. These measurements mapping frictional coefficients to load for each finger pad were recorded and fit to an inverse power law common to the soft elastic materials artificial finger pads nominally are fabricated from [19-21].

A. Key Parameters and Experimental Model

Elastically deformable objects create a variety of contact area geometry and pressure distributions depending on the object's initial geometry, the loading and the half space the object is in contact with [9]. We selected three common primitive finger pad geometries used in research and commercial hands: a cube, a cylinder and a sphere, and modeled those geometries as a single finger pad in contact with a normal planar half space "surface". These finger pad geometries create unique contact areas (square, rectangle, and circle) and unique pressure distributions when loaded onto an elastic or rigid half space [9]. Assuming a point load centered on the finger pad, elastic cubic objects distribute the loading pressure heavily towards the edges whereas elastic spherical objects distribute pressure towards the middle of the contact surface area. A cylinder is a mix of these two geometries and creates a pressure that distributes force toward the center of the rounded profile and towards the edges of the cylinder length [9]. We would like to experimentally determine how different key variables, including the loading magnitude, contact geometry and contact area, vary parameters that are key to robotic grasping applications.

Due to the variability in gripper kinematics, architecture, and object geometry seen in robotic grasping applications, we simplified our experimental framework to model the
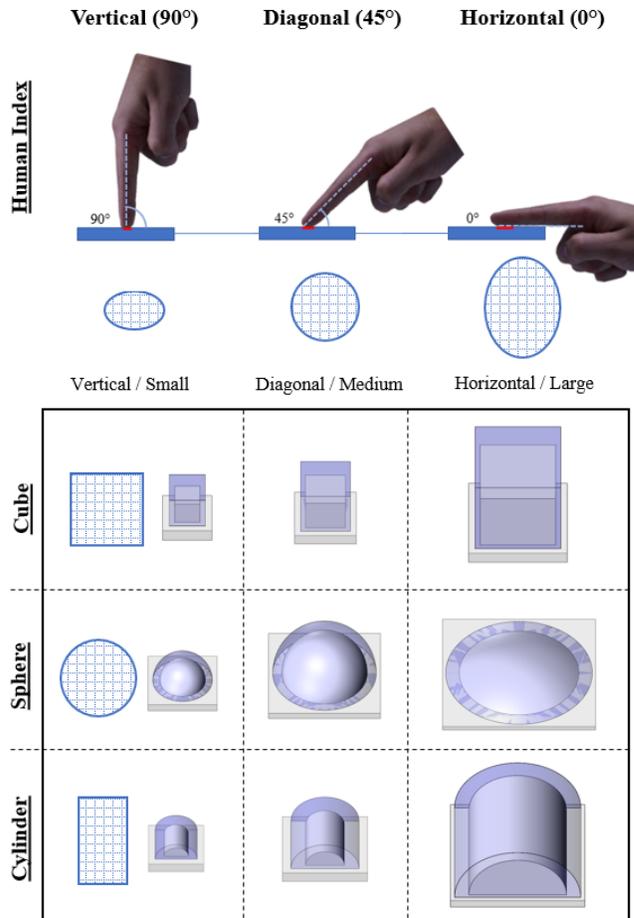

Figure 2. *Above:* The human index finger surface area measured in three orientations – vertical (90°), diagonal (45°) and horizontal (0°) – resembling three different contact area geometries and magnitudes. *Below:* The cubic, spherical and cylindrical fabricated finger pad primitive geometries in three sizes that provided identical contact area to the human index finger in three different orientations or small, medium and large.

interaction of a single finger pad and a flat rigid half space. Although this model may be simple, we believe it is an accurate representation of a generic grasping scenario between a digit in a multi-fingered hand and the face of an object. When determining whether an object can be grasped by an elastic finger pad, one must ensure that the force is exerted within the friction cone. The larger the friction cone, the more likely the given kinematics of a hand-object system can produce a stable grasp across antipodal points [4]. We assume a simple Coulomb model of friction where the holding force $F_{Friction}$ is less than or equal to the coefficient of friction μ multiplied by the normal force F_{Normal} while the pad and object are static. Similarly, the object and fingertip begin stably sliding when the holding force equates to the coefficient of friction multiplied by the normal force.

$$F_{Friction} \leq \mu_{Static} F_{Normal} \qquad (1)$$

$$F_{Friction} = \mu_{Kinetic} F_{Normal} \qquad (2)$$

For elastic structures such as Silicone and the human finger pad, tribological literature describes the coefficient of friction as nonlinear, varying in a negative power law relationship
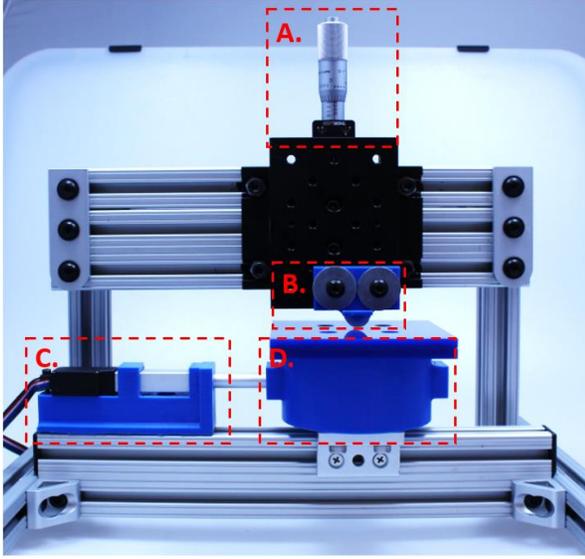
Figure 3. Testing apparatus for the friction testing including a vertical axis driven by a micrometer (A) that loads the mounted grip pad (B) into a rigid surface. That surface is driven orthogonally across the grip pad by a linear actuator (C) and the loading and frictional forces are recorded by a six-axis load cell (D).

with the applied normal force [19-21]. This deviation from Admontons' laws of friction states that there are nonlinear variations of the coefficient of friction with surface area and applied loads for elastic deformable materials.

$$\mu_{Static} = a(F_{Normal})^{n-1} \quad (3)$$

Where a and n are constants and the coefficient of friction decreases with applied load for flat rigid surfaces. Additionally, the surface level effect of adhesion, $F_{Adhesive}$, also provides the ability to add to the normal force and is observed for different surface materials, temperatures, humidity and pressure variations [19]. In this paper, we characterize this adhesive force as being influenced by our design variables (geometry, pressure) while minimizing effects from variations in materials, temperature and humidity. Under this model, finger pads with a higher coefficient of friction for a given surface area and loading are considered more effective because they create a wider friction cone, providing more holding force before slip and resistance to external wrenches after a successful grasp [4]. This holds for multi-fingered systems commonly seen in robotic grasping, however, other kinematic properties such as force direction at contact, antipodal point locations and caging configurations can alter grasp performance.

$$\mu_{Static} - \tan(\theta_{obj}) \leq \frac{|F_{cy}|}{|F_{cx}|} \leq \mu_{Static} + \tan(\theta_{obj}) \quad (4)$$

$$P_{F-O} = \frac{F_{Normal}}{A_{Contact}} \quad (5)$$

Where μ_{Static} is the static coefficient of friction, F_{cx} and F_{cy} are the x and y components of the contact force and θ_{obj} is the relative orientation of the object and the applied force. Because our test setup is a single finger pad that is

orthogonally loaded, we can assume that the θ_{obj} is zero and that the contact holding pressure, P_{F-O}, is equal to the normal force divided by the finger pad contact area, $A_{Contact}$.

B. Fabrication of Primitive Finger Pads

A pipeline was created to measure the human index finger pad contact area in the horizontal, diagonal and vertical positions under a common loading to provide three unique target contact surface areas for the artificial primitive geometries (Fig. 2). Although there is a sufficient amount of information available when it comes to the frictional properties of the human finger pad [19][22-23], the exact relationships between finger orientation and loads that we are interested in for robotic grasping were not comprehensibly reported. While the peak grasp force of the human hand can be more than 75N [24], we decided on a common loading of 12.5N or approximately half the nominal force output of the human finger force across all ages [25]. The finger pads contact area were equated at a single loading force because it would be impossible to equate a sphere, which converges to a point contact at arbitrarily low force, to a cylinder, converging to a line contact, and a cube, converging to a surface. Thus, when comparing lower forces, we can assume contact area does vary between the finger pads, however, minimal contact area variation will occur for loads higher than the common load assuring there is no plastic deformation or yielding. It is noted that the normalized contact area could have been any arbitrary area, however, we aimed to create finger pads with easily relatable geometries, rigidity and thickness that allow us to compare and contrast them from the human finger pad.

A single participant with approximately a 50th percentile male sized hand transferred his fingerprint (EZ ID #3 Ink) to a graph paper on top of a load cell. The applied loading force was gradually increased in real time until the loading threshold was met. A custom orthosis with a digital angle gauge (Wixey Digital Angle Gauge) was attached to the finger to ensure the correct orientation (0°, 45°, 90°) was maintained during contact and loading. This graph paper was then scanned in high resolution and the ink finger print was isolated from the background grid. The grid lines were used to normalize the pixel width to millimeters allowing us to calculate the area using the prints convex hull because all three orientations provided fingerprints that were ovular and convex in shape as seen in Figure 2. Each finger orientation was recorded one hundred times and the average surface areas were recorded in Table 1.

A similar pipeline was used to create the nine artificial finger pads consisting of three primitive geometries at the three predetermined contact areas. The artificial finger pads were fabricated out of a silicone rubber (Smooth-On Dragonskin 30A) that is a similar durometer to the human finger pad [26] and the surface was a quarter inch acrylic (PMMA). A single combination of object and finger pad material were selected to maintain a consistent relationship between coefficients of friction during testing. The thickness of the pads varied based on size, with the large pad resembling the horizontal orientation at 4mm thick, the medium pad at 3mm thick and the small pad at 2mm thick to resemble the

distal human finger pad [27]. Each finger pad was experimentally evaluated using the fingerprint loading pipeline above until the surface area fell within 5% of the estimated human index contact area for each given orientation. The finger pads were then characterized by their largest linear dimension. The cubic finger pads are characterized by side length *L,* the spherical finger pads by the diameter *D,* and the cylindrical finger pads by the diameter *D* that was set equal to the length *L* for this study. The nine finger pads were each molded directly onto a rigid mounting block that was screwed onto the testing apparatus described in the next section (Fig. 3). It is noted that the vertical edges for the cube and cylinder edges were only one millimeter thick to mitigate excessive deflection of the pad while sliding and the cylindrical and spherical pads were created in halves so that they could be more easily mounted to the loading axis. We believe that these modifications improved the consistency of the kinetic and static coefficients of friction during testing.

C. Testing Procedure

A testing apparatus was developed to align with the ASTM D1894 standard providing guidelines for evaluating the effective static and kinetic coefficients of friction for thin elastic materials. Although this standard is not explicitly designed for the evaluation of artificial finger pads, we found it to be the closest fit for our testing. The sphere was slid in a single direction, the cube was slid along its edge and the cylinder was tested in both the radial and axial directions. We established five loads that are representative of robotic grasping conditions to evaluate the static and kinetic coefficients of friction for the primitive robotic finger pads. The chosen loading magnitudes describe full force (25N), half-force (12.5) and low-force (1N, 2N, 5N) measurements relative to estimated human finger force production [25]. The low force range of 2N and 5N were recorded because they are critical for determining the power law relationship between loading and coefficient of friction seen in the human finger and elastic materials [19]. It is noted that although these normal loads are representative of robotic grasping, the finger pads were only loaded vertically and do not have the same force-position relationships as a normal robotic hand.

For a given trial, the finger pad was mounted to a mechanical optical micrometer with high resolution and a normal load was applied to a quarter inch thick acrylic sheet that was mounted on a six-axis load cell (ATI). The load was applied gradually to minimize viscoelastic effects and the micrometer stage was locked before sliding was forced. A linear actuator (Firgelli L12-50-210) was used to horizontally drive the loaded acrylic surface mounted on low friction rails across the finger pads. The linear actuator was driven at a load exceeding the static friction limit at the ASTM prescribe rate of 150 mm/sec. This fast driving rate helped avoid stick-slip behavior improving the isolation and classification of the coefficient of kinetic friction. We confirmed that the linear actuator was strong enough for the vertical loading to have negligible effects on the sliding rate of the acrylic surface. The static friction coefficient was determined as the maximum ratio between the frictional and loading force. The kinetic friction coefficient was the average ratio between holding and
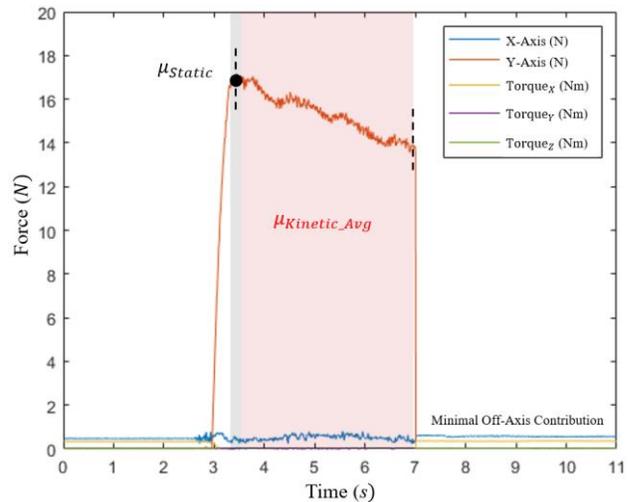

Figure 4.   Trial of an artificial cubic finger pad loaded to 25N and forced into y-direction sliding. Following the ASTM standard and constant loading force, the static coefficient of friction was determined at the peak frictional force and the kinetic was calculated as the average frictional force during stable sliding which was determined visually.

loading force while the pad was stably sliding over the surface (Fig. 4). These calculations and more details on the testing procedures are described in [18].

Additional precautions were taken above the ASTM standards when preparing the robotic geometric primitives and test setup. First, the room temperature and humidity was recorded because it had a significant effect on the coefficient of friction for smooth materials [21-23]. The testing was completed in a climate-controlled room with minimal variance in temperature and humidity. Next, before each primitive was tested, both the acrylic half space and primitive surface were cleaned with a 70/30 isopropyl alcohol solution to remove any dust or surface contaminants. The pads were molded with a smooth molding surface (Stratasys Objet30 Pro VeroClear) to ensure consistency and to remove ridges that occur from machined or FDM 3D printed molds. Last, the pads were removed after molding and adhered with a specialty super glue (Loctite 4471) designed with high shear strength to mitigate variations in pad adhesion to the supporting 3d printed chassis.

III. RESULTS

A. Determining Finger Pad Contact Area

To normalize the contact surface area of the fabricated primitives, the contact area of the human index finger of a single participant (Male 26, approx. 50th percentile male [28]) was used under a common load of 12.5N in the horizontal, diagonal and vertical orientations. The measured horizontal, or finger in plane with the surface contact, surface area was 311.11 mm^2 with a standard deviation of 17.96 mm^2. The measured diagonal, or finger 45 degrees offset from the surface plane, contact area was 103.14 mm^2 with a standard deviation of 10.81 mm^2. The measured vertical, or the finger 90 degrees offset from the surface plane, contact area was 60.12 mm^2 with a standard deviation of 4.61 mm^2. All three contact geometries were ovular, the horizontal orientation

TABLE I.   FINGER PAD SURFACE AREA AT 12.5N CONTACT

| Pad Type	Contact Surface Area by Orientation		
	Horizontal (0° x 4mm)	*Diagonal (45° x 3mm)*	*Vertical (90° x 2mm)*
Human Index	A = 311.11 mm^2 σ = 17.96 mm^2	A = 103.14 mm^2 σ = 10.81 mm^2	A = 60.12 mm^2 σ = 4.61 mm^2
Cube	A = 315.48 mm^2 σ = 12.84 mm^2 L = 17.02 mm	A = 109.60 mm^2 σ = 5.94 mm^2 L = 10.41 mm	A = 60.00 mm^2 σ = 5.72 mm^2 L = 6.86 mm
Sphere	A = 304.52 mm^2 σ = 20.34 mm^2 D = 129.54 mm	A = 107.74 mm^2 σ = 2.41 mm^2 D = 35.31 mm	A = 59.35 mm^2 σ = 4.34 mm^2 D = 17.53 mm
Cylinder	A = 300.64 mm^2 σ = 17.33 mm^2 L=D = 35.8 mm	A = 100.00 mm^2 σ = 3.14 mm^2 L=D = 14.22 mm	A = 58.06 mm^2 σ = 1.02 mm^2 L=D = 9.65 mm
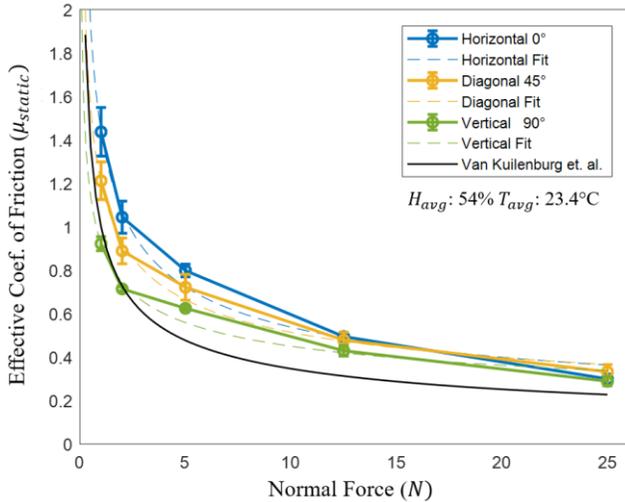
Figure 5.   Evaluation of the variation of static coefficient of friction with the normal loading force for the human index finger in the three loading orientations. The negative power law relationship is compared to a meta study of the human finger provided in [19].

largest linear dimension is in the y-axis, the diagonal orientation approximately circular and the vertical orientation largest linear dimension is in the x-axis (Fig. 2). The surface area and largest linear dimension for the human index finger and fabricated primitive finger pads are recorded in Table 1.

The fabrication of the final nine finger pads for testing were revised until their contact areas were within one standard deviation of the human index finger contact area (F_N = 12.5N, $n_{samples}$ = 100) . This deviation was to account for variations from the molding and loading process such as air bubbles and slight variations in thickness. The final finger pads largest linear dimensions (LLD) were recorded in the horizontal orientation (large), diagonal orientation (medium) and vertical orientation (small) in Table 1. To produce a given contact area, the sphere required the largest linear dimension followed by the cylinder then the square which required the smallest linear dimension. The spherical pad was so much larger than the other pads for a given contact area that in order to produce the contact area of the human index finger at 0° (~25mm LLD) under 12.5 N of loading the sphere would have to have five times the LLD whereas the cube would only require two thirds the LLD. These linear dimension

relationships agree with current hertzian theory seen in [9] given the L=D assumption for our cylinder geometry.

B.   Evaluating Key Grasping Parameters

The effective coefficient of friction for the human index finger was recorded in different orientations under different loading magnitudes. We found that at lower loads the coefficient of friction differed visibly based on orientation with the coefficient of friction increasing with surface area. For the lowest load of 1N, the horizontal orientation had a coefficient of friction of $\mu_{HI\_0°}$ = 1.437, the diagonal orientation with $\mu_{HI\_45°}$ = 1.212 and the vertical orientation with $\mu_{HI\_90°}$ = 0.922. At the higher normal forces we observed that orientation and contact area had less of an effect on the coefficient of friction at 12.5N ($\mu_{HI\_0°}$ = 0.494, $\mu_{HI\_45°}$ = 0.473, $\mu_{HI\_90°}$ = 0.429) and at 25N ($\mu_{HI\_0°}$ = 0.300, $\mu_{HI\_45°}$ = 0.332, $\mu_{HI\_90°}$ = 0.289). The highest average deviation across normal force levels was recorded for the diagonal orientation and the lowest average deviation for the vertical orientation. We found that the human index finger tested using the ASTM D1894 standard followed a similar power law to that recorded in a meta study [19] which averaged the coefficient of friction of the human finger under varying loading conditions, orientations, surface moisture and surface materials (Fig. 5).

The artificial finger pads displayed rather different power law relationships between the applied normal load and coefficients of friction. The cubic contact geometry observed the highest coefficient of friction at a low load (1N) as indicated by *a* in Table 2. The spherical and cylindrical transverse observed a similar coefficient of friction with axial sliding producing a slightly higher coefficient at low loads. This indicates that there could be a friction benefit when sliding axially versus transverse with a cylindrical finger pad. The power law coefficient *n* was formed such that as the load increased the coefficients of friction monotonically decreased in a non-linear fashion until converged to similar coefficients at higher loads. The only outliers were the 0° (large) and 45° (medium) cubic finger pads that displayed slightly elevated coefficients at the higher loads. This indicates that a cubic geometry and square contact area may be favorable to generate a higher coefficient of friction under most grasping loads for a flat surface. We observed smaller variance in the artificial finger pad coefficient variance than in the human finger coefficients which we believe is due to slight inconsistencies while loading and positioning the finger and finger pad moisture.

When measuring the differences between static and kinetic coefficients, the cubic grip pad had the largest difference for $\mu_{K\_Cube\_0°}$ = 2.491 or only 41% of the static coefficient at the lowest load. This was consistent for all the artificial finger pads that recorded larger differences between the static and kinetic coefficients in the lower normal force range. Conversely, for higher normal forces we observed smaller differences in static and kinetic coefficients for all finger pads. On average, the kinetic coefficient of friction was 60.4% static for 1N and 93.5% static for 25N loading across all geometries. The artificial finger pad with the smallest nominal difference between static and kinetic coefficients of

TABLE II.   FRICTION CHARACTERISTICS FOR ROBOTIC FINGER PADS

Pad Type	Effective Coefficient of Friction			Power Law Coefficients	
	1 N	12.5 N	25 N	Static	Kinetic
Cube 0°	μ_S= 6.10 μ_K= 2.50	μ_S= 1.71 μ_K= 1.49	μ_S= 1.17 μ_K= 1.09	a =6.159 n =0.462	a =2.534 n =0.756
Cube 45°	μ_S= 3.87 μ_K= 1.90	μ_S= 0.78 μ_K= 0.70	μ_S= 0.62 μ_K= 0.58	a =3.794 n =0.361	a =1.931 n =0.361
Cube 90°	μ_S= 1.67 μ_K= 1.04	μ_S= 0.49 μ_K= 0.43	μ_S= 0.33 μ_K= 0.30	a =1.688 n =0.534	a =1.056 n =0.634
Sphere 0°	μ_S= 2.99 μ_K= 1.99	μ_S= 1.11 μ_K= 0.97	μ_S= 0.85 μ_K= 0.82	a =2.994 n =0.594	a =2.039 n =0.722
Sphere 45°	μ_S= 1.56 μ_K= 1.03	μ_S= 0.58 μ_K= 0.51	μ_S= 0.43 μ_K= 0.41	a =1.635 n =0.615	a =1.045 n =0.711
Sphere 90°	μ_S= 1.16 μ_K= 0.82	μ_S= 0.45 μ_K= 0.40	μ_S= 0.32 μ_K= 0.30	a =1.163 n =0.627	a =0.789 n =0.694
Cyl. T. 0°	μ_S= 2.72 μ_K= 1.71	μ_S= 1.11 μ_K= 1.00	μ_S= 0.80 μ_K= 0.75	a =2.933 n =0.681	a =1.763 n =0.760
Cyl. T. 45°	μ_S= 1.90 μ_K= 1.29	μ_S= 0.64 μ_K= 0.58	μ_S= 0.44 μ_K= 0.42	a =1.929 n =0.563	a =1.270 n =0.663
Cyl. T. 90°	μ_S= 1.42 μ_K= 0.90	μ_S= 0.44 μ_K= 0.38	μ_S= 0.31 μ_K= 0.29	a =1.412 n =0.529	a =0.887 n =0.642
Cyl. A 0°	μ_S= 3.17 μ_K= 1.71	μ_S= 1.12 μ_K= 1.03	μ_S= 0.83 μ_K= 0.80	a =3.209 n =0.593	a =1.720 n =0.783
Cyl. A 45°	μ_S= 1.52 μ_K= 0.99	μ_S= 0.50 μ_K= 0.45	μ_S= 0.37 μ_K= 0.34	a =1.545 n =0.568	a =0.983 n =0.693
Cyl. A 90°	μ_S= 1.30 μ_K= 0.72	μ_S= 0.36 μ_K= 0.31	μ_S= 0.26 μ_K= 0.24	a =1.283 n =0.466	a =0.719 n =0.664

friction was the sphere with 83% and the primitive with the largest nominal difference was the cube with 76%. When the static and kinetic coefficients are similar it is difficult to determine whether or not the finger is frictionally sliding, frictionally sticking or rapidly transitioning between the two [18]. This required us to complete more tests at the higher loads to find areas where we could observe stable sliding. Although we observed minimal variance in finger pad coefficient measurement, we believe the higher nominal variance in kinetic coefficients over static occurred from difficulties in determining stable sliding.

The effective "holding pressure" was measured as the holding force divided by the contact area and was larger for the smaller finger pads for each given geometry (Fig. 6). The effective holding pressure of the smallest finger pads and index in the vertical orientation under this loading was similar, measured at approximately 0.090 N/mm². For the largest contact area finger pads, the Cubic finger pads had the highest holding pressure, measured at 0.068 N/mm², the spherical and cylindrical finger pads were in the middle, measured at approximately 0.046 N/mm², and the human finger horizontal orientation had the lowest, measured at 0.020 N/mm². Holding forces were measured to determine the relative holding force, at which the object shears from the hand, of the finger pads for use in a robotic gripper. Variations of this holding force with area, benefits of higher and lower coefficients of friction and practical design insight using these experimental parameters will be discussed in the next section.

IV. DISCUSSION

A. Performance of Artificial Primitive Finger Pads

We set forth to evaluate simple artificial primitive finger pads made of silicone rubber by varying applied loading, contact area and contact geometry. We defined an effective single contact as one that would produce that largest coefficient of friction and holding pressure between the hand-object system. A larger static coefficient of friction correlates to a larger frictional or holding force before slip occurs for a generic contact assuming minimal variation in adhesive forces between the finger and object [4]. We observed that the cube had the highest coefficient of friction for all three orientations. We expect our power law extrapolation to hold for higher forces until the elastic material yields, however, at forces lower than 1N we would expect this trend to round off as the cylinder and sphere converge to a line or point contact. This inverse power law relationship indicates that coefficient of friction is not constant during grasping, especially in the low force ranges as the object is being acquired. The relationships between normal load and surface traction presented can bolster models for the motion planning and manipulation communities, that are presented tasks that require repetitive grasping or grasps with varying force.

At 12.5N loading force, where the pads have almost identical surface areas, we observed that all the robotic primitives monotonically increased in holding force with an increase in surface area. The human finger had only a small increase in holding force with surface area with 5.4N for the vertical orientation and 6.2N for the horizontal orientation. The largest increase was for the cubical finger pads with 6.2N holding force in the vertical orientation and 21.4N of holding force in the horizontal orientation. Higher holding force for a given loading force is favorable in robotic grasping tasks because it requires less electromechanical power for an equivalent grasp. Along with maximizing holding force for a given applied load, another important metric to designers is to maximize the holding force relative to the finger pad size.
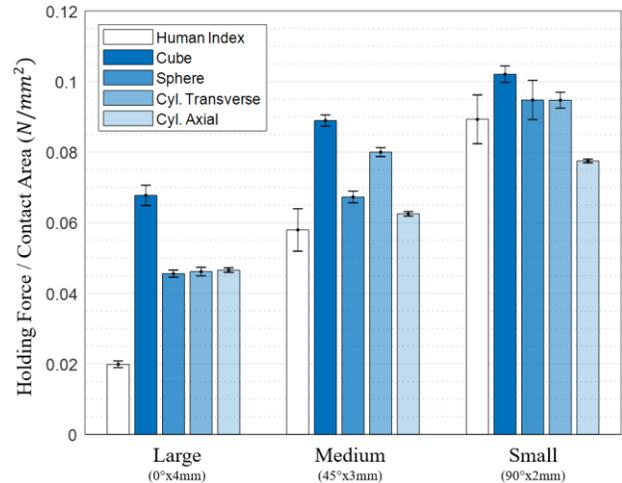

Figure 6.   Comparison of the holding pressure for three size pads for each of the three fabricated finger pad primitive geometries and the human finger. This was defined as the lateral force required to overcome static friction divided by the contact surface area for all of the finger pad sizes.

Having excessively large finger pads affects the weight, packaging and maximum object size that can be grasped for a given kinematic architecture. We defined this aspect "packaging" and evaluated it by normalizing the frictional holding force of each pad by its largest linear dimension, providing a ratio between the compactness and grasping effectiveness of the finger pad. This analysis further favored the cubic grip pads that were relatively compact with high coefficients of friction and disfavored the larger spherical pads. When evaluating the "packaging" of each of the three sizes for the geometric primitives, smaller grip pads outperformed larger pads for the spherical and cylindrical pads while the cubic pads remained fairly similar across orientations. Due to the diminishing returns, smaller grip pads could be optimal for grasping conditions that are compact and higher frictional forces are not required. Relevant applications include small surgical grippers, precision grippers, fingertips, hands that require multiple points of contact and caging grippers.

All three finger pads were deemed more effective for robotic grasping applications over that of the human finger in this test setup. We believe this was an artifact of the surface moisture, human finger ridges and the propensity to resist injury. As an additional analysis, we wanted to compare the required normal force the artificial pad's gripper would have to maintain to exert a similar frictional force to the human finger. The only grip pad configuration that was unable to equate to the human finger pad in our test setup was the smallest surface area cylinder in the axial orientation under the 12.5N and 25N loadings in which the value was comparable. The cube performed the best only requiring 1.53N of loading force to output the same frictional force of the human finger with 25N loading. The largest sphere and cylinder also performed well, requiring from two to four times less normal force to provide the same frictional force as the human finger. This implies that for smooth dry surfaces grip pads are more efficient than the human finger for grasping.

B. Design Guidelines for Simple Robotic Finger Pads

In examining the results, we can see several performance advantages from the primitive geometries that could be useful for engineers wanting to design simple and effective robotic finger pads. First, the cubic finger pad observed favorable frictional, shear and holding force performance at low forces and we believe this is due to the finger pad's relatively even distribution of pressure spawning from matching finger pad and surface geometry. Being able to produce a high holding force at a low load is critical for grasping applications so that the object does not reconfigure or slip as it is being acquired. Next, as the geometry of the finger pad moves further from that of the surface, the pressure becomes more concentrated towards the areas of initial contact and therefore slip initiates on the lower pressure areas. For the simple geometries studied here, the pressure concentration relates to the nature of the contact in the un-deformed state or in a very low force state: a surface contact for the cube, a line contact for the cylinder, or a point contact for the sphere. The closer the finger pad geometry matches the geometry of the surface, the more equal the pressure distribution and the better the frictional performance. This infers that flat finger pads will perform best on flat surfaces, given that they are closely aligned in orientation, and curved pads on curved surfaces with very similar curvature. In summary, when designing finger pads, one should not only match curvature but also avoid variations in thickness of the pad where low pressure areas may develop when in contact with an object. We foresee a combination of curvature and thickness variation as an ideal solution to developing a simple grip pad for a given application. In future research, we would like to evaluate the performance of simple finger pads under more complex loading conditions and object geometries.

Our previous analysis focused on maximizing the frictional properties of a single contact on a flat surface, however, most practical robotic grippers are far more complex. Applying this idea to practical hands and grasping scenarios, flat finger pads
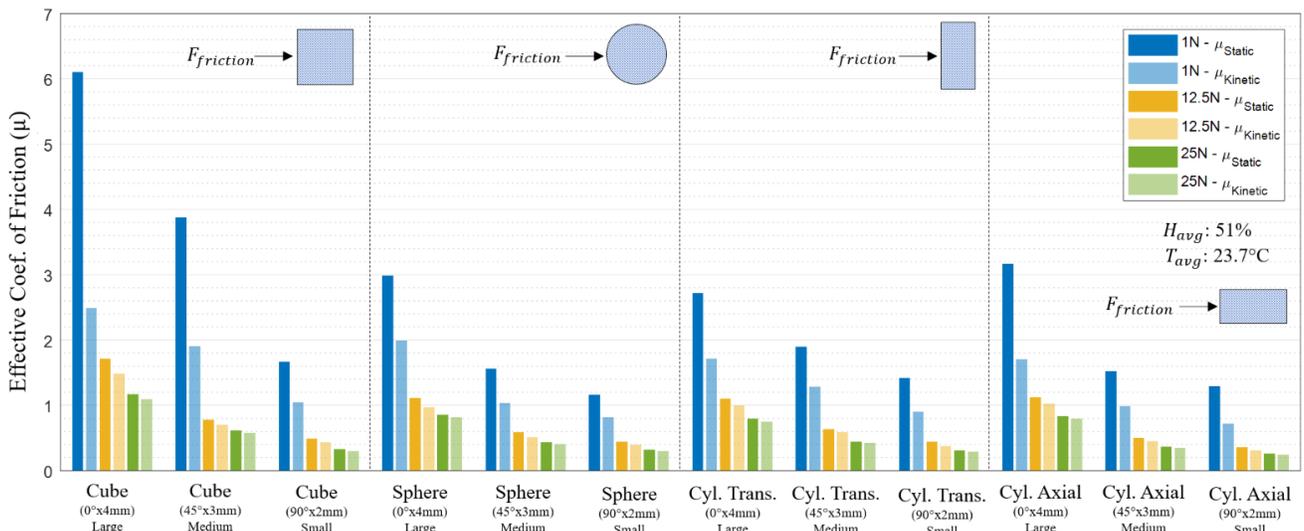

Figure 7. Evaluation of the variation in the effective static and kinetic coefficients of friction relative to a low (1N), medium (12.5N) and high (25N) normal loading force for the fabricated finger pad primitives. The three primitive geometries grip pads are listed in descending order from the pad of that geometry with the largest contact area and displacement to the smallest contact area and displacement. The cylinder is evaluated in two sliding modes, one sliding across the cylinder round or transverse direction and one sliding across the cylinder length or axial direction.

are generally only going to align well to flat surfaces in planar graspers, especially parallel jaw grippers. Most other hand-object configurations that rely on several contacts will produce several line contacts or point contacts. For these scenarios, which represent the vast majority of cases for prosthesis, it is therefore best practice to attempt to increase the radius of the finger pad at the regions of expected contact to be as large as is reasonable, assuming the contacted surface is locally convex. If contact happens on a sharp edge (e.g. the edge of a polyhedron or the leading edges of a cylinder) a near zero-radius contact region will form producing unfavorable holding force and frictional properties. Thus, we recommend that finger pads should be "rounded off" with the largest reasonable radius for their application to mitigate unfavorable contact locations at the pad limits. We recommend this for prosthesis and other multi-finger robotic grasping applications where object uncertainty can force contact in unfavorable locations. If significant uncertainty is expected, one could take this concept to the limits by creating a reasonably sized spherical surface that will provide minimal frictional benefits, however, ensure the object will contact the finger pad away from boundaries and in a predictable manner.

There are some applications where both being able to grasp and then manipulate an object are desired, either with multiple fingers or a single finger and the support plane. This typically involves some amount of pivoting of the object with respect to the initial contact location and surfaces. In these cases, some amount of rolling is typically required and if the contact location is a sharp point contact (of very small or zero radius) the rolling of the object will likely not produce significant contact location changes. This will allow for more free motion because the structure of the fingertip will provide very few constraints to rotation. Thus, a sphere, although slightly underperforming in frictional characteristics, is a favorable contact geometry when designing for manipulation because it allows for more mobility of the object at the contact and a somewhat reliable knowledge of the contact center of rotation for post contact planning. An additional possibility to solving both surface alignment and manipulation issues is to have a simple passively reorienting finger pad that self-aligns with local geometry, allowing slip during manipulation and maximizing contact area passively post-manipulation [11]. In the future, we want to further investigate the combination simple finger pad geometries (cube, cylinder, sphere) and smart finger design to maximize the ability for a robotic finger to not only grasp but manipulate an object.

References

[1] J.K. Salisbury. "The design and control of a dexterous mechanical hand." *Proc. ASME Computer Conf.*, USA, 1981.

[2] R.R. Ma, N. Rojas and A.M. Dollar. "Spherical Hands: Towards Underactuated, In-Hand Manipulation Invariant to Object Size and Grasp Location." *ASME Journal of Mechanisms and Robotics*, 2016.

[3] Robotiq Hand-E, 2-Finger and 3-Finger Adaptive Robot Grippers, 2019. https://robotiq.com/products/3-finger-adaptive-robot-gripper

[4] C. Piazza, G. Grioli, M.G. Catalano and A. Bicchi. "A Century of Robotic Hands." *Annual Review of Control, Robotics and Autonomous Systems*, Vol. 2, No. 1, pp.1-32, 2019.

[5] L. Birglen, T. Laliberte and C.M. Gosselin. *Underactuated Robotic Hands*. Springer-Verlag, 2008.

[6] M. Roa and R. Suarez. "Grasp quality measures: review and performance." *Autonomous Robots*, Vol. 38, pp.65-88, 2015.

[7] H. Hertz. "On the contact of solid elastic bodies and on hardness." *Journal of Math*, Vol. 92, pp.156-171, 1881.

[8] R. Mindlin. "Compliance of elastic bodies in contact." *Journal of Applied Mechanics*, Vol. 16, pp.259-268, 1949.

[9] K.L. Johnson. *Contact Mechanics*. Cambridge University Press, 1985.

[10] H.X. Trinh, V.A. Ho and K. Shibuya. "Theoretical Foundation for Design of Friction-Tunable Soft Finger with Wrtinkle's Morphology." *IEEE Robotics and Automation Letters*, 2019.

[11] R.R. Ma, N. Rojas and A.M. Dollar. "Towards Predicable Precision Manipulation of Unknown Objects with Underactuated Fingers." *Advances in Reconfigurable Mechanisms and Robots II*, Vol.36, pp.927-937, 2016.

[12] M. Honarpardaz, M. Tarkain, D. Sirkett, J. Olvander, X. Feng, J. Elf and R. Sjogren. "Generic Automated Multi-Function Finger Design." *International Conference on Mechanical Engineering and Automation Science*, 2016.

[13] M. Li, K. Hang, D. Kragic and A. Billard. "Dexterous Grasping Under Shape Uncertainty." *Robotics and Autonomous Systems*, Vol. 75, pp. 352-364, 2016.

[14] J. Mahler, J. Liang, S. Niyaz, M. Laskey, R. Doan, X. liu, J. Ojea and K. Goldberg. "Dex-Net 2.0: Deep Learning to Plan Robust Grasps with Synthetics Point Clouds and Analytic Grasp Metrics." *Robotics: Science and Systems*, 2017.

[15] B. Calli, A. Walsman, A. Singh, S. Srinivasa, P. Abbeel and A. Dollar. "Benchmarking in Manipulation Research: The YCB Object and Model Set and Benchmarking Protocols." *IEEE Robotics and Automation Magazine*, Vol. 22, No. 3, pp. 36-52, 2015.

[16] H. Song, M. Wang and K. Hang. "Fingertip Surface Optimization for Robust Grasping on Contact Primitives." *IEEE Robotics and Automation Letters*, Vol.3, No. 2, pp.742-749, 2018.

[17] F. Chen, W. Xu, H. Zhang, Y. Wang, J. Cao, M.Y. Wang, H. Ren, J. Zhu and Y.F. Zhang. "Topology Optimized Design, Fabrication, and Characterization of a Soft Cable-Driven Gripper." *IEEE Robotics and Automation Letters*, Vol. 3, No. 3, pp. 2463-2470, 2018.

[18] ASTM Standard D1894, 2001, "Standard Test Method for Static and Kinetic Coefficients of Friction of Plastic Film and Sheeting," ASTM International, West Conshohocken, PA, USA. www.astm.org.

[19] J. Van Kuilenburg, M.A. Masen and E. Van Der Heide. "A review of fingerpad contact mechanics and friction and ahow this affects tactile perception." *J. Engineering Tribology*, Vol. 229, pp.243-258, 2015.

[20] H. Han, A. Shimada and S. Kawamura. "Analysis of Friction on Human Fingers and Design of Artificial Fingers." *IEEE Int. Conf. on Robotics and Automation*, Minnesota, USA, 1996.

[21] N. Nachman and S.E. Franklin. "Artificial skin model simulating dry and moist *in vivo* human skin friction and deformation behavior." *Tribology International*, Vol. 97, pp.431-439, 2016.

[22] C.P. Hendriks and S.E. Franklin. "Influence of surface roughness, material and climate conditions on the friction of human skin." *Tribology Letters*, Vol. 37 pp. 361-373, 2010.

[23] M. Klaassen, E.G. De Vries and M.A. Masen. "Friction in the contact between skin and a soft counter material: effects of hardness and surface finish." *Journal of the Mechanical Behavior of Biomedical Materials*, Vol. 92, pp. 137-143, 2019.

[24] V. Mathiowetz, N. Kashman, G. Volland, K. Weber, M. Dowe and S. Rogers. "Grip and Pinch Strength: Normative Data for Adults." *Arch. Phys. Med. Rehabilitation*, Vol. 66, pp. 69-72, 1985.

[25] R.W. Gregory. "Biomechanics and Control of Torque Production During Prehension" PhD Diss., Pennsylvania State University, 2002.

[26] V. Falanga and B. Bucalo. "Use of durometer to assess skin hardness." *Journal of the American Academy of Dermatology*, Vol. 29, No. 1, pp. 47-51, 1993.

[27] H. Bruhn, M. Gyngell, W. Hanicke, K. Merboldt and J. Frahm. "High-resolution fast low-angle shot magnetic resonance imaging of the normal hand." *Skeletal Radiology*, Vol, 20, pp. 259-265, 1991.

[28] A.R. Tilley. *The Measure of Man and Woman: Human Factors in Design*, John Wiley and Sons, New York, 2002.